


Andreev reflection spectroscopy in strongly paired superconductorsCyprian Lewandowski ^{1,2,*}, Étienne Lantagne-Hurtubise ^{1,2}, Alex Thomson,^{1,2,3,4}
Stevan Nadj-Perge ^{2,5} and Jason Alicea ^{1,2}¹*Department of Physics, California Institute of Technology, Pasadena, California 91125, USA*²*Institute for Quantum Information and Matter, California Institute of Technology, Pasadena, California 91125, USA*³*Walter Burke Institute for Theoretical Physics, California Institute of Technology, Pasadena, California 91125, USA*⁴*Department of Physics, University of California, Davis, California 95616, USA*⁵*T. J. Watson Laboratory of Applied Physics, California Institute of Technology,
1200 East California Boulevard, Pasadena, California 91125, USA* (Received 25 July 2022; revised 29 October 2022; accepted 13 December 2022; published 6 January 2023)

Motivated by recent experiments on low-carrier-density superconductors, including twisted multilayer graphene, we study signatures of the BCS-to-BEC evolution in Andreev reflection spectroscopy. We establish that in a standard quantum point contact geometry, Andreev reflection in a BEC superconductor is unable to mediate a zero-bias conductance beyond e^2/h per lead channel. This bound is shown to result from a mapping that links the subgap conductance of BCS and BEC superconductors. We then demonstrate that sharp signatures of BEC superconductivity, including perfect Andreev reflection, can be recovered by tunneling through a suitably designed potential well. We propose various tunneling spectroscopy setups to experimentally probe this recovery.

DOI: [10.1103/PhysRevB.107.L020502](https://doi.org/10.1103/PhysRevB.107.L020502)

Introduction. The evolution from Bardeen-Cooper-Schrieffer (BCS) to Bose-Einstein condensate (BEC) superconductivity has been a recurring theme in the study of physical systems ranging from cold atomic gases to strongly correlated materials and neutron stars [1–5]. In the BCS regime, superconductivity arises from weakly bound Cooper pairs with a characteristic size ξ_{pair} that far exceeds the mean interparticle spacing d ; in the BEC regime, by contrast, fermions form tightly bound Cooper pairs with size $\xi_{\text{pair}} \ll d$. BCS- and BEC-type superconductors can be separated either by a crossover [e.g., for s -wave pairing [6–11]; Fig. 1(a)], a Lifshitz-type phase transition [e.g., for nodal pairing [12–14]; Fig. 1(b)], or a topological phase transition [15].

Ultracold atoms, where the pairing strength between fermions can be continuously tuned with the aid of a Feshbach resonance [16,17], provide a controlled experimental platform for exploring the evolution from weak to strong pairing in both three [18–23] and two [24–30] spatial dimensions. While most solid-state superconductors reside firmly in the BCS regime, certain strongly correlated materials such as cuprates have been rationalized in terms of the BCS-BEC paradigm [31] (see, however, Ref. [32]). Further, a new generation of experiments probing low-carrier-density materials including iron-based compounds [33–36], Li_xZrNCl [37–39], and moiré graphene systems [40–45] has revealed signatures consistent with proximity to a BEC state—opening a new experimental frontier for unconventional superconductivity. Developing probes that can unambiguously identify BEC

superconductors and distinguish possible competing phases therefore poses a pressing problem.

In solid-state contexts, BEC superconductivity can manifest in various ways. Saturation of the Ginzburg-Landau coherence length ξ_{GL} at the interparticle spacing [37,40] and a critical temperature approaching theoretical bounds [46,47] both constitute indirect evidence for proximity to the strong pairing regime. Energy-momentum-resolved probes [34] can also reveal the evolution of the quasiparticle dispersion from BCS-like to BEC-like [Figs. 1(a) and 1(b)]. Superconductors with a nodal order parameter exhibit a Lifshitz transition from a gapless BCS to a gapped BEC phase, which leads to a predicted divergence in electronic compressibility at the transition [13] and a gap opening that can be observed, e.g., via scanning tunneling microscopy (STM) [12,14,42]. In STM it is, however, difficult to distinguish BEC superconductors from competing insulators since, unlike their BCS counterparts, they feature less prominent and particle-hole asymmetric coherence peaks [42,48].

Here, we investigate Andreev reflection spectroscopy across the BCS-BEC evolution and predict striking manifestations of BEC superconductivity. First, in a standard quantum point contact (QPC) geometry [49] we find that Andreev reflection is suppressed upon passing from the BCS to the BEC regime, consistent with the analysis of BEC-BEC Josephson junctions in Ref. [50]. We show that this suppression is a consequence of a mapping that interchanges the wave functions of BEC and BCS superconductors. Second, we establish that Andreev reflection can be controllably revived in the BEC regime by tunneling between the lead and superconductor through an effective potential *well*—as opposed to the barrier employed in conventional treatments [51]. This feature sharply distinguishes BEC from BCS superconductors

*clewandowski@magnet.fsu.edu

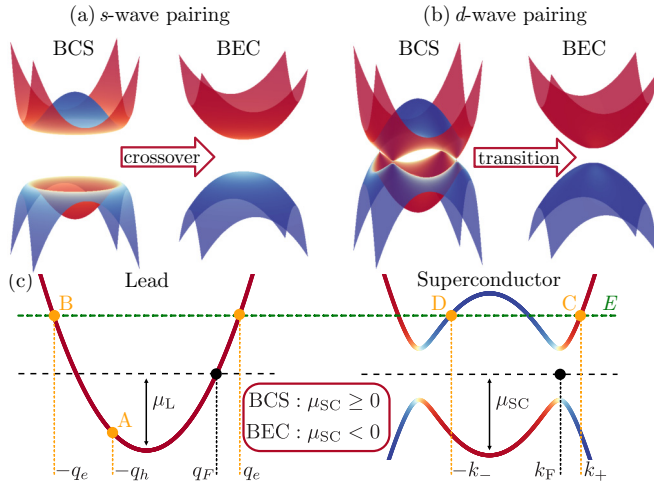


FIG. 1. (a), (b) Quasiparticle spectra across the BCS-to-BEC superconductor evolution, which is (a) a crossover for s -wave pairing but (b) a Lifshitz transition for nodal (e.g., d -wave) pairing. (c) Scattering processes at the normal-superconductor interface included in the BTK formalism: Andreev (A) and normal (B) reflection, and direct (C) and band-crossing (D) transmission as a quasiparticle. The green dashed line denotes the incident electron energy.

and can be probed in experimental setups that we propose.

Setup. We first employ the Blonder-Tinkham-Klapwijk (BTK) framework, which describes scattering between a normal lead and a superconductor [51]. Consider a one-dimensional (1D) setup [Fig. 1(c)] with an interface at position $x = 0$ separating a spinful normal lead (at $x < 0$) with dispersion $\xi_q = \frac{q^2}{2m_L} - \mu_L$ from a singlet superconductor (at $x > 0$) with dispersion $\xi_k = \frac{k^2}{2m_{SC}} - \mu_{SC}$ and s -wave pairing potential Δ . We take $\mu_L > 0$ throughout but allow μ_{SC} to take either sign to capture the BCS-BEC crossover that occurs as μ_{SC} crosses zero [52]. A delta-function tunnel barrier $\lambda\delta(x)$ interpolates between the tunneling limit with large $\lambda > 0$ and the QPC limit $\lambda = 0$.

Figure 1(c) illustrates the processes available to an incident electron at the interface: Andreev (A) or normal (B) reflection to a hole or electron, respectively, and transmission to an electron- (C) or holelike (D) quasiparticle. The probabilities for these processes are obtained by matching the wave functions and their first derivatives at the interface and normalizing by the appropriate group velocities (see Supplemental Material [53] for details of the calculation and Ref. [54]). In the standard BTK formalism applied to weakly paired BCS superconductors, the limit $\Delta, E \ll \mu_L, \mu_{SC}$ combined with the equal-mass assumption $m_L = m_{SC}$ drastically simplifies the problem, yielding the Andreev approximation in which $q_h = q_e = k_{\pm} = q_F$ with $q_F = \sqrt{2m_L\mu_L}$ the lead's Fermi momentum [55]. To describe the BCS-BEC evolution, we instead treat the problem in full generality (see Ref. [50] for an analogous treatment of Josephson junctions). The tunneling conductance $G(E) = dI/dV$ at bias energy $E = eV$ is given in the Landauer-Büttiker formalism by

$$G(E) = \frac{2e^2}{h} [1 + A(E) - B(E)], \quad (1)$$

where $A(E)$ and $B(E)$ denote the Andreev and normal reflection probabilities. Maximal conductance of $4e^2/h$ corresponds to perfect Andreev reflection $A(E) = 1$.

Zero-bias conductance. For gapped superconductors, the absence of transmission processes (C and D) considerably simplifies the analysis of the subgap conductance: Employing the normalization condition $A(E) + B(E) = 1$ returns $G(E) = \frac{4e^2}{h} A(E)$. As shown in the Supplemental Material [53], the zero-bias Andreev reflection probability $A_0 \equiv A(E = 0)$ then reduces to

$$A_0 = \frac{4v_L^2 v_1^2}{[(2v_L Z + v_R)^2 + v_1^2 + v_L^2]^2}, \quad (2)$$

where $Z = \lambda/v_L$ quantifies the barrier transparency, $v_L = q_F/m_L$ is the Fermi velocity of the lead, and $v_{R,I} = \kappa_{R,I}/m_{SC}$ are two characteristic velocities of the superconductor. The momenta $\kappa_{R,I}$ are defined through

$$\kappa e^{i\varphi} = \kappa_R + i\kappa_I = \sqrt{2m_{SC}(-\mu_{SC} + i\Delta)}, \quad (3)$$

and the length scales κ_R^{-1} and κ_I^{-1} respectively control the evanescent and oscillatory behavior of the wave function in the superconductor at $x > 0$, $\psi_{SC} \sim e^{-(\kappa_R + i\kappa_I)x}$.

Sending $\mu_{SC} \rightarrow -\mu_{SC}$, which connects the BCS and BEC regimes, yields $\varphi \rightarrow \pi/2 - \varphi$ and hence swaps $\kappa_R \leftrightarrow \kappa_I$; cf. Eq. (3). This remarkable property reveals a mapping between the BCS and BEC superconductor wave functions. As an instructive limiting case, deep in either the BEC or BCS regimes where $|\mu_{SC}|/\Delta \gg 1$, $\kappa_{R,I}$ can be expanded as

$$\kappa_R + i\kappa_I \approx \sqrt{\text{sgn}(\mu_{SC})} \left(\frac{\Delta}{v_F} + i \text{sgn}(\mu_{SC}) k_F \right), \quad (4)$$

where $k_F = \sqrt{2m_{SC}|\mu_{SC}|}$ and $v_F = k_F/m_{SC}$. In the BCS limit Eq. (4) aligns with conventional understanding: The wave function's oscillatory part is set by the Fermi momentum k_F , whereas evanescent decay is controlled by Δ/v_F —i.e., the inverse of the BCS pair coherence length ξ_{pair} . The situation flips in the BEC regime, where k_F , which can be interpreted as the inverse scattering length of the pairing potential [4], controls the decay length and Δ/v_F dictates the oscillatory behavior.

This mapping has immediate implications for the conductance. In the QPC limit, $Z = 0$, the Andreev reflection probability in Eq. (2) is maximized when the lead Fermi velocity satisfies $v_L = \sqrt{v_R^2 + v_1^2}$, yielding the upper bound $A_0 \leq v_1^2/(v_1^2 + v_R^2)$ valid for any μ_{SC} . Near-perfect Andreev reflection thus requires $v_R \ll v_1$, implying many oscillation periods over the decaying envelope of the superconductor wave function. This requirement exactly translates to the BCS limit, $\mu_{SC} \gg \Delta$, as originally pointed out by Andreev [55]. By contrast, the deep BEC regime is characterized by the converse inequality $v_R \gg v_1$, and the upper bound above accordingly reduces to $A_0 \lesssim v_1^2/v_R^2 = \Delta^2/\mu_{SC}^2$. Physically, the fast decay of the superconducting wave function relative to its oscillation period suppresses Andreev reflection from the plane-wave electrons of the lead. At the “self-dual” point $\mu_{SC} = 0$, the superconductor exhibits a single length scale, with $v_R = v_1 = \sqrt{\Delta/m_{SC}}$, yielding an Andreev reflection probability upper-bounded by 1/2.

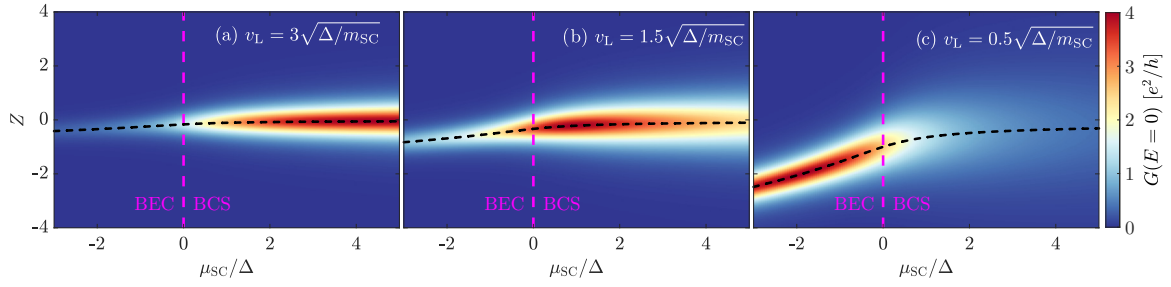


FIG. 2. Dependence of the BTK zero-bias tunneling conductance on the barrier parameter Z along the BCS-to-BEC crossover for a one-dimensional s -wave superconductor with $v_L\sqrt{m_{SC}}/\Delta$ set to (a) 3, (b) 1.5, and (c) 0.5. Black dashed lines trace $Z = -v_R/2v_L$, one of the necessary conditions for perfect Andreev reflection. Incoming electrons tunnel through a potential barrier at $Z > 0$ but a potential well at $Z < 0$. While the conductance in the BCS regime is approximately $Z \rightarrow -Z$ symmetric, pronounced asymmetry emerges in the BEC regime, with enhanced Andreev reflection possible at negative Z [see (c)].

Andreev revival. The preceding bound on Andreev reflection in the BEC regime ($\mu_{SC} < 0$) implies that the zero-bias conductance in the QPC limit cannot exceed the value $2e^2/h$ characteristic of a perfect metallic contact. According to Eq. (2), moving away from the QPC limit by adding a tunnel barrier modeled by $Z > 0$ only further suppresses the Andreev reflection probability A_0 . Interestingly, however, Andreev reflection can be enhanced by exploiting a pronounced asymmetry in the sign of Z that emerges in the BEC regime.

Writing $v_l = \alpha v_L$ and $v_R = \beta v_L$, one can reexpress Eq. (2) as $A_0 = 1/(1 + \tilde{Z}^2)^2$ in terms of a renormalized transparency parameter,

$$\tilde{Z}^2 = \frac{(Z + \beta/2)^2}{\alpha} + \frac{(\alpha - 1)^2}{4\alpha}, \quad (5)$$

that incorporates both the intrinsic barrier transparency Z and velocity mismatch effects (see Supplemental Material [53] and also Ref. [56]). The linear-in- Z contribution in Eq. (5) is proportional to the dimensionless parameter $\beta/\alpha = v_R/v_l$ controlling the BEC-to-BCS evolution. In the BCS limit, the distinction between Z positive and negative—i.e., potential barriers and wells—is correspondingly negligible since $v_l \gg v_R$. In the BEC regime, by contrast, $v_R > v_l$ implies sensitive dependence on the sign of Z . Indeed, potential wells characterized by $Z < 0$ can promote Andreev reflection—which becomes perfect at zero bias even deep within the BEC regime when $\tilde{Z} = 0$, i.e., when $Z = -v_R/(2v_L)$ and $v_L = v_l$. These trends are illustrated in Fig. 2, which plots the zero-bias conductance versus Z across the BCS-BEC evolution tuned by μ_{SC}/Δ , for different lead velocities v_L in Figs. 2(a)–2(c). Note that the standard BTK result for a BCS superconductor is recovered for large v_L [Fig. 2(a)].

Effective lead formalism. For complementary insight, we now examine normal metal-superconductor tunneling via an effective lead formalism (ELF). Consider a 1D lead at positions $x \leq 0$ with linearized kinetic energy and Fermi velocity $v_L = q_F/m_L$. At its endpoint, the lead exhibits a local potential $U_0\delta(x)$ and couples to a gapped d -dimensional superconductor via electron hopping of strength t ; see Fig. 3. Focusing on subgap energies, the superconductor’s degrees of freedom can be safely integrated out—yielding an effective lead-only Hamiltonian with additional (marginal) “impurity” perturbations (see Supplemental Material [53] for details of the calculation and Ref. [57]). Specifically, the

superconductor both shifts the local potential U_0 by

$$U_{SC} = t^2 \int \frac{d^d \mathbf{k}}{(2\pi)^d} \frac{\xi_{\mathbf{k}}}{\xi_{\mathbf{k}}^2 + \Delta^2} \quad (6)$$

and generates a local singlet pairing term with amplitude

$$W_{SC} = t^2 \int \frac{d^d \mathbf{k}}{(2\pi)^d} \frac{\Delta}{\xi_{\mathbf{k}}^2 + \Delta^2}. \quad (7)$$

Explicit evaluation of the integrals reveals that, for $d = 1$, U_{SC} and W_{SC} exactly swap under $\mu_{SC} \rightarrow -\mu_{SC}$, manifesting the mapping uncovered above within the BTK formalism. [We note that Eq. (6) diverges for dimensions $d = 2, 3$ and a UV cutoff has to be introduced. For further discussion and extensions, see Supplemental Material [53].]

Extracting the wave functions from the effective lead-only Hamiltonian yields a zero-bias Andreev reflection probability [53]

$$A_0^{\text{ELF}} = \frac{4v_L^2(W_{SC}/2)^2}{[(U_{\text{eff}}/2)^2 + (W_{SC}/2)^2 + v_L^2]^2}, \quad (8)$$

with $U_{\text{eff}} = U_0 + U_{SC}$. Equation (8) reproduces Eq. (2) upon identifying the ELF/BTK correspondence $U_0/2 \leftrightarrow 2v_L Z$, $U_{SC}/2 \leftrightarrow v_R$, and $W_{SC}/2 \leftrightarrow v_l$. Thus negative values of U_0 enable the cancellation of the “large” potential U_{SC} generated by BEC superconductors, in turn allowing Andreev processes mediated by W_{SC} to dominate.

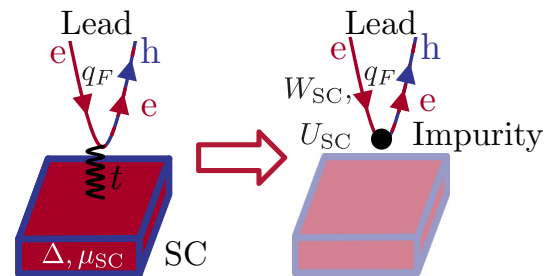


FIG. 3. Sketch of the effective lead formalism. A lead tunnels electrons onto a gapped superconductor (left). Integrating out the gapped degrees of freedom generates an effective lead-only “impurity” problem (right) featuring a shifted local potential U_{SC} and a local pairing term W_{SC} mediated by the superconductor.

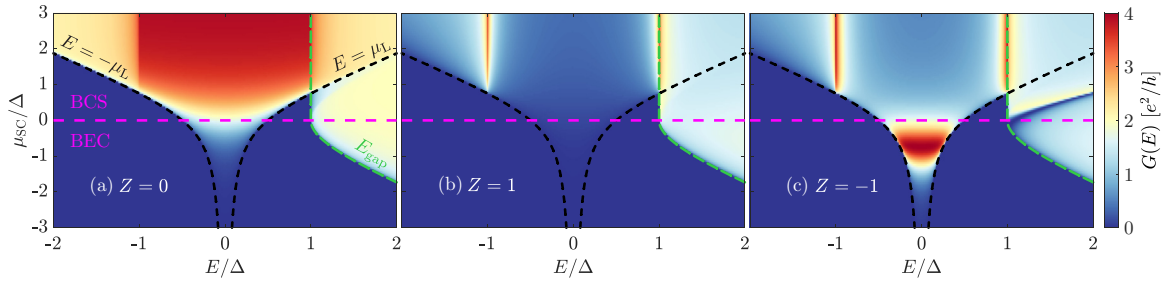


FIG. 4. Finite-bias tunneling spectroscopy across the BCS-BEC evolution with (a) $Z = 0$, (b) $Z = 1$, and (c) $Z = -1$, assuming an optimal lead with $v_L = v_I$ for each μ_{SC} value. Black dashed lines at energies $E = \pm\mu_L$ show the corresponding optimal lead chemical potential μ_L , and green dashed lines denote the quasiparticle gap E_{gap} . (a) The quantum point contact limit $Z = 0$ exhibits a plateau-like enhancement of subgap conductance due to the Andreev reflection in the BCS regime, but not in the BEC regime. (b), (c) Tunneling spectra for $Z = \pm 1$ are similar in the BCS regime, showing a gap surrounded by coherence peaks at $E = \pm\Delta$. In the BEC regime, subgap conductance enhancement occurs *only* for tunneling through potential wells, as in (c).

Extensions. Figure 4 presents the finite-bias conductance $G(E)$ for an s -wave superconductor. Data were obtained numerically from the full BTK analysis, including quasiparticle transmission channels, for $Z = 0$ [Fig. 4(a)], (b) $Z = 1$ [Fig. 4(b)], and $Z = -1$ [Fig. 4(c)]. To clearly illustrate the revival of Andreev reflection, the lead Fermi velocity is tuned such that $v_L = v_I$ across the BCS-BEC evolution; that is, for each μ_{SC} on the vertical axis we fix the lead chemical potential to its optimal value (see dashed black curves). In the QPC limit, $Z = 0$, Fig. 4(a) shows the familiar subgap conductance plateau at $G(E) = 4e^2/h$ in the BCS regime [51]. Upon entering the BEC regime, the entire plateau is suppressed in accordance with the bound on Andreev reflection at zero bias derived above. In the tunneling limit ($Z > 0$), the BCS regime exhibits sharp coherence peaks at the gap edge that similarly diminish upon entering the BEC regime, as shown in Fig. 4(b). Finally, negative Z continues to support coherence peaks in the BCS regime while also significantly enhancing the subgap conductance in the BEC regime [Fig. 4(c)]. This enhancement is present within an energy interval about zero bias whose extent is limited by kinematic constraints imposed by the lead chemical potential μ_L (the required backwards propagating hole state does not exist for $|E| > \mu_L$).

Our 1D analysis extends to the experimentally relevant scenario of a multichannel lead normally incident on a 2D superconductor (see Supplemental Material [53] and also Ref. [58]). In the limit of many ballistic channels, the total conductance $G(E)$ follows from an angular average over the contributions from all momenta in the plane of the interface [49,53,59,60]. For isotropic s -wave superconductors this procedure leads to essentially identical results as in our 1D model. Nodal superconductors also show qualitatively similar “revival” behavior at negative Z in the BEC regime; the key distinguishing feature is that subgap conductance generated by Andreev reflection in the BCS regime acquires an inverted V shape [59] due to transmission processes that suppress Andreev reflection away from zero bias [53].

Discussion. The suppression of Andreev reflection in a quantum point contact geometry, and its recovery by tunneling through potential wells, clearly differentiates BEC phenomenology from the familiar properties of BCS superconductors (and, of course, from insulators). In partic-

ular, the emergence of a pronounced $Z \rightarrow -Z$ asymmetry in the subgap conductance provides a striking signature of BEC superconductivity. This feature stands in stark contrast to the above-gap conductance $G(E \gg \Delta)$ that is manifestly symmetric with respect to the sign of Z [53]. Possible experimental setups for probing the negative- Z regime include (i) scanning tunneling spectroscopy (STS) measurements using a tip with an effective quantum well at its end, implemented by attaching, e.g., a quantum dot (reminiscent of single-electron transistor probes [61,62]) or an impurity atom, or else by coating the tip with a layer of material with a smaller work function and (ii) 2D electronic transport setups where the normal-superconductor (N-S) interface is tunable, either by applying a local gate near the junction or by constructing “via contacts” etched into different encapsulating insulators [63]. The latter experimental geometry is of particular interest as it allows, in principle, to tune v_L *in situ* and thus realize the optimal regime for Andreev reflection $v_L \approx v_I$.

Throughout this Letter we focused on superconductivity arising from a single parabolic band. Extending these ideas to BEC physics in multiband superconductors, believed to be important to understanding recent experiments [34], is thus warranted. The limit of narrow-band superconductivity, where quantum geometry plays an important role in determining the superfluid stiffness [43,64–69], is another interesting avenue for future work with possible applications to moiré materials [40–42]. Finally, self-consistent treatments and extensions beyond mean field [10,11,70–79] might lead to further insights into BEC superconductors and associated pseudogap physics at temperatures above T_c .

Acknowledgments. We thank Mohit Randeria, Hyunjin Kim, Michał Papaj, and Kevin Nuckolls for insightful discussions. This work was supported by the Gordon and Betty Moore Foundation’s EPiQS Initiative, Grant No. GBMF8682 (C.L. and É.L.-H.); the U.S. Army Research Office under Grant Award No. W911NF-17-1-0323 (J.A.); the Caltech Institute for Quantum Information and Matter, an NSF Physics Frontiers Center with support of the Gordon and Betty Moore Foundation through Grant No. GBMF1250 (J.A. and S.N.-P.); the NSF Career programme (DMR-1753306) (S.N.-P.); and the Walter Burke Institute for Theoretical Physics at Caltech (A.T. and J.A.).

- [1] Q. Chen, J. Stajic, S. Tan, and K. Levin, BCS-BEC crossover: From high temperature superconductors to ultracold superfluids, *Phys. Rep.* **412**, 1 (2005).
- [2] C. A. S. de Melo, When fermions become bosons: Pairing in ultracold gases, *Phys. Today* **61**(10), 45 (2008).
- [3] W. Zwerger, *The BCS-BEC Crossover and the Unitary Fermi Gas*, Lecture Notes in Physics Vol. 836 (Springer, Berlin, 2011).
- [4] M. Randeria and E. Taylor, Crossover from Bardeen-Cooper-Schrieffer to Bose-Einstein condensation and the unitary Fermi gas, *Annu. Rev. Condens. Matter Phys.* **5**, 209 (2014).
- [5] G. C. Strinati, P. Pieri, G. Röpke, P. Schuck, and M. Urban, The BCS-BEC crossover: From ultra-cold Fermi gases to nuclear systems, *Phys. Rep.* **738**, 1 (2018).
- [6] D. M. Eagles, Possible pairing without superconductivity at low carrier concentrations in bulk and thin-film superconducting semiconductors, *Phys. Rev.* **186**, 456 (1969).
- [7] A. Leggett, *Modern Trends in the Theory of Condensed Matter: Proceedings of the XVI Karpacz Winter School of Theoretical Physics*, edited by A. Pekalski and J. Przystawa, Lecture Notes in Physics Vol. 115 (Springer, Berlin, 1980).
- [8] P. Nozières and S. Schmitt-Rink, Bose condensation in an attractive fermion gas: From weak to strong coupling superconductivity, *J. Low Temp. Phys.* **59**, 195 (1985).
- [9] M. Randeria, J.-M. Duan, and L.-Y. Shieh, Bound States, Cooper Pairing, and Bose Condensation in Two Dimensions, *Phys. Rev. Lett.* **62**, 981 (1989).
- [10] C. A. R. Sá de Melo, M. Randeria, and J. R. Engelbrecht, Crossover from BCS to Bose Superconductivity: Transition Temperature and Time-Dependent Ginzburg-Landau Theory, *Phys. Rev. Lett.* **71**, 3202 (1993).
- [11] F. Pistolesi and G. C. Strinati, Evolution from BCS superconductivity to Bose condensation: Calculation of the zero-temperature phase coherence length, *Phys. Rev. B* **53**, 15168 (1996).
- [12] M. Randeria, J.-M. Duan, and L.-Y. Shieh, Superconductivity in a two-dimensional Fermi gas: Evolution from Cooper pairing to Bose condensation, *Phys. Rev. B* **41**, 327 (1990).
- [13] R. D. Duncan and C. A. R. Sá de Melo, Thermodynamic properties in the evolution from BCS to Bose-Einstein condensation for a d -wave superconductor at low temperatures, *Phys. Rev. B* **62**, 9675 (2000).
- [14] L. Borkowski and C. S. de Melo, Evolution from the BCS to the Bose-Einstein limit in a d -wave superconductor at $t = 0$, *Acta Phys. Pol. A* **99**, 691 (2001).
- [15] N. Read and D. Green, Paired states of fermions in two dimensions with breaking of parity and time-reversal symmetries and the fractional quantum Hall effect, *Phys. Rev. B* **61**, 10267 (2000).
- [16] S. Giorgini, L. P. Pitaevskii, and S. Stringari, Theory of ultracold atomic Fermi gases, *Rev. Mod. Phys.* **80**, 1215 (2008).
- [17] C. Chin, R. Grimm, P. Julienne, and E. Tiesinga, Feshbach resonances in ultracold gases, *Rev. Mod. Phys.* **82**, 1225 (2010).
- [18] C. A. Regal, M. Greiner, and D. S. Jin, Observation of Resonance Condensation of Fermionic Atom Pairs, *Phys. Rev. Lett.* **92**, 040403 (2004).
- [19] M. W. Zwierlein, C. A. Stan, C. H. Schunck, S. M. F. Raupach, A. J. Kerman, and W. Ketterle, Condensation of Pairs of Fermionic Atoms near a Feshbach Resonance, *Phys. Rev. Lett.* **92**, 120403 (2004).
- [20] C. Chin, M. Bartenstein, A. Altmeyer, S. Riedl, S. Jochim, J. H. Denschlag, and R. Grimm, Observation of the pairing gap in a strongly interacting Fermi gas, *Science* **305**, 1128 (2004).
- [21] T. Bourdel, L. Khaykovich, J. Cubizolles, J. Zhang, F. Chevy, M. Teichmann, L. Tarruell, S. J. J. M. F. Kokkelmans, and C. Salomon, Experimental Study of the BEC-BCS Crossover Region in Lithium 6, *Phys. Rev. Lett.* **93**, 050401 (2004).
- [22] G. B. Partridge, K. E. Strecker, R. I. Kamar, M. W. Jack, and R. G. Hulet, Molecular Probe of Pairing in the BEC-BCS Crossover, *Phys. Rev. Lett.* **95**, 020404 (2005).
- [23] M. W. Zwierlein, J. R. Abo-Shaeer, A. Schirotzek, C. H. Schunck, and W. Ketterle, Vortices and superfluidity in a strongly interacting Fermi gas, *Nature (London)* **435**, 1047 (2005).
- [24] A. T. Sommer, L. W. Cheuk, M. J. H. Ku, W. S. Bakr, and M. W. Zwierlein, Evolution of Fermion Pairing from Three to Two Dimensions, *Phys. Rev. Lett.* **108**, 045302 (2012).
- [25] V. Makhalov, K. Martiyanov, and A. Turlapov, Ground-State Pressure of Quasi-2D Fermi and Bose Gases, *Phys. Rev. Lett.* **112**, 045301 (2014).
- [26] M. G. Ries, A. N. Wenz, G. Zürn, L. Bayha, I. Boettcher, D. Kedar, P. A. Murthy, M. Neidig, T. Lompe, and S. Jochim, Observation of Pair Condensation in the Quasi-2D BEC-BCS Crossover, *Phys. Rev. Lett.* **114**, 230401 (2015).
- [27] P. A. Murthy, I. Boettcher, L. Bayha, M. Holzmann, D. Kedar, M. Neidig, M. G. Ries, A. N. Wenz, G. Zürn, and S. Jochim, Observation of the Berezinskii-Kosterlitz-Thouless Phase Transition in an Ultracold Fermi Gas, *Phys. Rev. Lett.* **115**, 010401 (2015).
- [28] I. Boettcher, L. Bayha, D. Kedar, P. A. Murthy, M. Neidig, M. G. Ries, A. N. Wenz, G. Zürn, S. Jochim, and T. Enss, Equation of State of Ultracold Fermions in the 2D BEC-BCS Crossover Region, *Phys. Rev. Lett.* **116**, 045303 (2016).
- [29] K. Fenech, P. Dyke, T. Peppler, M. G. Lingham, S. Hoinka, H. Hu, and C. J. Vale, Thermodynamics of an Attractive 2D Fermi Gas, *Phys. Rev. Lett.* **116**, 045302 (2016).
- [30] L. Sobirey, N. Luick, M. Bohlen, H. Biss, H. Moritz, and T. Lompe, Observation of superfluidity in a strongly correlated two-dimensional Fermi gas, *Science* **372**, 844 (2021).
- [31] N. Harrison and M. K. Chan, Magic Gap Ratio for Optimally Robust Fermionic Condensation and its Implications for High- T_c Superconductivity, *Phys. Rev. Lett.* **129**, 017001 (2022).
- [32] J. Sous, Y. He, and S. A. Kivelson, Absence of a BCS-BEC crossover in the cuprate superconductors, [arXiv:2210.13478](https://arxiv.org/abs/2210.13478).
- [33] S. Kasahara, T. Watashige, T. Hanaguri, Y. Kohsaka, T. Yamashita, Y. Shimoyama, Y. Mizukami, R. Endo, H. Ikeda, K. Aoyama, T. Terashima, S. Uji, T. Wolf, H. von Löhneysen, T. Shibauchi, and Y. Matsuda, Field-induced superconducting phase of FeSe in the BCS-BEC cross-over, *Proc. Natl. Acad. Sci. USA* **111**, 16309 (2014).
- [34] S. Rinott, K. B. Chashka, A. Ribak, E. D. L. Rienks, A. Taleb-Ibrahimi, P. L. Fevre, F. Bertran, M. Randeria, and A. Kanigel, Tuning across the BCS-BEC crossover in the multiband superconductor $\text{Fe}_{1+y}\text{Se}_x\text{Te}_x$: An angle-resolved photoemission study, *Sci. Adv.* **3**, e1602372 (2017).
- [35] T. Hashimoto, Y. Ota, A. Tsuzuki, T. Nagashima, A. Fukushima, S. Kasahara, Y. Matsuda, K. Matsuura, Y. Mizukami, T. Shibauchi, S. Shin, and K. Okazaki, Bose-Einstein condensation superconductivity induced by

- disappearance of the nematic state, *Sci. Adv.* **6**, eabb9052 (2020).
- [36] Y. Mizukami, M. Haze, O. Tanaka, K. Matsuura, D. Sano, J. Böker, I. Eremin, S. Kasahara, Y. Matsuda, and T. Shibauchi, Thermodynamics of transition to BCS-BEC crossover superconductivity in $\text{FeSe}_{1-x}\text{S}_x$, [arXiv:2105.00739](https://arxiv.org/abs/2105.00739).
- [37] Y. Nakagawa, Y. Kasahara, T. Nomoto, R. Arita, T. Nojima, and Y. Iwasa, Gate-controlled BCS-BEC crossover in a two-dimensional superconductor, *Science* **372**, 190 (2021).
- [38] T. Shi, W. Zhang, and C. A. R. S. de Melo, Density-induced BCS-Bose evolution in gated two-dimensional superconductors: The role of the interaction range in the Berezinskii-Kosterlitz-Thouless transition, *Europhysics Lett.* **139**, 36003 (2022).
- [39] M. Heyl, K. Adachi, Y. M. Itahashi, Y. Nakagawa, Y. Kasahara, E. J. W. List-Kratochvil, Y. Kato, and Y. Iwasa, Vortex dynamics in the two-dimensional BCS-BEC crossover, *Nat. Commun.* **13**, 6986 (2022).
- [40] J. M. Park, Y. Cao, K. Watanabe, T. Taniguchi, and P. Jarillo-Herrero, Tunable strongly coupled superconductivity in magic-angle twisted trilayer graphene, *Nature (London)* **590**, 249 (2021).
- [41] Z. Hao, A. M. Zimmerman, P. Ledwith, E. Khalaf, D. H. Najafabadi, K. Watanabe, T. Taniguchi, A. Vishwanath, and P. Kim, Electric field-tunable superconductivity in alternating-twist magic-angle trilayer graphene, *Science* **371**, 1133 (2021).
- [42] H. Kim, Y. Choi, C. Lewandowski, A. Thomson, Y. Zhang, R. Polski, K. Watanabe, T. Taniguchi, J. Alicea, and S. Nadj-Perge, Evidence for unconventional superconductivity in twisted trilayer graphene, *Nature (London)* **606**, 494 (2022).
- [43] H. Tian, S. Che, T. Xu, P. Cheung, K. Watanabe, T. Taniguchi, M. Randeria, F. Zhang, C. N. Lau, and M. W. Bockrath, Evidence for flat band Dirac superconductor originating from quantum geometry, [arXiv:2112.13401](https://arxiv.org/abs/2112.13401).
- [44] J. M. Park, Y. Cao, L.-Q. Xia, S. Sun, K. Watanabe, T. Taniguchi, and P. Jarillo-Herrero, Robust superconductivity in magic-angle multilayer graphene family, *Nat. Materials* **21**, 877 (2022).
- [45] Y. Zhang, R. Polski, C. Lewandowski, A. Thomson, Y. Peng, Y. Choi, H. Kim, K. Watanabe, T. Taniguchi, J. Alicea, F. von Oppen, G. Refael, and S. Nadj-Perge, Promotion of superconductivity in magic-angle graphene multilayers, *Science* **377**, 1538 (2022).
- [46] S. S. Botelho and C. A. R. Sá de Melo, Vortex-Antivortex Lattice in Ultracold Fermionic Gases, *Phys. Rev. Lett.* **96**, 040404 (2006).
- [47] T. Hazra, N. Verma, and M. Randeria, Bounds on the Superconducting Transition Temperature: Applications to Twisted Bilayer Graphene and Cold Atoms, *Phys. Rev. X* **9**, 031049 (2019).
- [48] Y. L. Loh, M. Randeria, N. Trivedi, C.-C. Chang, and R. Scalettar, Superconductor-Insulator Transition and Fermi-Bose Crossovers, *Phys. Rev. X* **6**, 021029 (2016).
- [49] D. Daghero and R. S. Gonnelli, Probing multiband superconductivity by point-contact spectroscopy, *Supercond. Sci. Technol.* **23**, 043001 (2010).
- [50] F. Setiawan and J. Hofmann, Analytic approach to transport in superconducting junctions with arbitrary carrier density, *Phys. Rev. Res.* **4**, 043087 (2022).
- [51] G. E. Blonder, M. Tinkham, and T. M. Klapwijk, Transition from metallic to tunneling regimes in superconducting microconstrictions: Excess current, charge imbalance, and supercurrent conversion, *Phys. Rev. B* **25**, 4515 (1982).
- [52] In this Letter we consider a sudden jump between the chemical potentials μ_L and μ_{SC} at the interface, which neglects possible electrostatic effects present at the interface (see, e.g., Ref. [78]).
- [53] See Supplemental Material at <http://link.aps.org/supplemental/10.1103/PhysRevB.107.L020502> for details of the BTK analysis and the ELF model, generalization to nodal pairing, and a discussion of tunneling with multiple channels.
- [54] R. C. Dynes, V. Narayanamurti, and J. P. Garno, Direct Measurement of Quasiparticle-Lifetime Broadening in a Strong-Coupled Superconductor, *Phys. Rev. Lett.* **41**, 1509 (1978).
- [55] A. Andreev, The thermal conductivity of the intermediate state in superconductors, *Sov. Phys. JETP* **19**, 1228 (1964).
- [56] S. Lee, V. Stanev, X. Zhang, D. Stasak, J. Flowers, J. S. Higgins, S. Dai, T. Blum, X. Pan, V. M. Yakovenko, J. Paglione, R. L. Greene, V. Galitski, and I. Takeuchi, Perfect andreev reflection due to the Klein paradox in a topological superconducting state, *Nature (London)* **570**, 344 (2019).
- [57] L. Fidkowski, J. Alicea, N. H. Lindner, R. M. Lutchyn, and M. P. A. Fisher, Universal transport signatures of Majorana fermions in superconductor-Luttinger liquid junctions, *Phys. Rev. B* **85**, 245121 (2012).
- [58] E. Lake, A. S. Patri, and T. Senthil, Pairing symmetry of twisted bilayer graphene: A phenomenological synthesis, *Phys. Rev. B* **106**, 104506 (2022).
- [59] S. Kashiwaya, Y. Tanaka, M. Koyanagi, and K. Kajimura, Theory for tunneling spectroscopy of anisotropic superconductors, *Phys. Rev. B* **53**, 2667 (1996).
- [60] D. Daghero, M. Tortello, P. Pecchio, V. A. Stepanov, and R. S. Gonnelli, Point-contact Andreev-reflection spectroscopy in anisotropic superconductors: The importance of directionality (review article), *Low Temp. Phys.* **39**, 199 (2013).
- [61] M. J. Yoo, T. A. Fulton, H. F. Hess, R. L. Willett, L. N. Dunkleberger, R. J. Chichester, L. N. Pfeiffer, and K. W. West, Scanning single-electron transistor microscopy: Imaging individual charges, *Science* **276**, 579 (1997).
- [62] J. Martin, N. Akerman, G. Ulbricht, T. Lohmann, J. H. Smet, K. von Klitzing, and A. Yacoby, Observation of electron-hole puddles in graphene using a scanning single-electron transistor, *Nat. Phys.* **4**, 144 (2008).
- [63] Q. Cao, E. J. Telford, A. Benyamini, I. Kennedy, A. Zangiabadi, K. Watanabe, T. Taniguchi, C. R. Dean, and B. M. Hunt, Tunneling spectroscopy of two-dimensional materials based on via contacts, *Nano Lett.* **22**, 8941 (2022).
- [64] S. Peotta and P. Törmä, Superfluidity in topologically nontrivial flat bands, *Nat. Commun.* **6**, 8944 (2015).
- [65] A. Julku, S. Peotta, T. I. Vanhala, D.-H. Kim, and P. Törmä, Geometric Origin of Superfluidity in the Lieb-Lattice Flat Band, *Phys. Rev. Lett.* **117**, 045303 (2016).
- [66] J. S. Hofmann, E. Berg, and D. Chowdhury, Superconductivity, pseudogap, and phase separation in topological flat bands, *Phys. Rev. B* **102**, 201112(R) (2020).
- [67] P. Törmä, S. Peotta, and B. A. Bernevig, Superconductivity, superfluidity and quantum geometry in twisted multilayer systems, *Nat. Rev. Phys.* **4**, 528 (2022).

- [68] A. Julku, G. M. Bruun, and P. Törmä, Quantum Geometry and Flat Band Bose-Einstein Condensation, *Phys. Rev. Lett.* **127**, 170404 (2021).
- [69] N. Verma, T. Hazra, and M. Randeria, Optical spectral weight, phase stiffness, and T_c bounds for trivial and topological flat band superconductors, *Proc. Natl. Acad. Sci. USA* **118**, e2106744118 (2021).
- [70] V. J. Emery and S. A. Kivelson, Importance of phase fluctuations in superconductors with small superfluid density, *Nature (London)* **374**, 434 (1995).
- [71] E. Taylor, A. Griffin, N. Fukushima, and Y. Ohashi, Pairing fluctuations and the superfluid density through the BCS-BEC crossover, *Phys. Rev. A* **74**, 063626 (2006).
- [72] H. Hu, X.-J. Liu, and P. D. Drummond, Equation of state of a superfluid Fermi gas in the BCS-BEC crossover, *Europhys. Lett.* **74**, 574 (2006).
- [73] N. Fukushima, Y. Ohashi, E. Taylor, and A. Griffin, Superfluid density and condensate fraction in the BCS-BEC crossover regime at finite temperatures, *Phys. Rev. A* **75**, 033609 (2007).
- [74] R. B. Diener, R. Sensarma, and M. Randeria, Quantum fluctuations in the superfluid state of the BCS-BEC crossover, *Phys. Rev. A* **77**, 023626 (2008).
- [75] G. Bertaina and S. Giorgini, BCS-BEC Crossover in a Two-Dimensional Fermi Gas, *Phys. Rev. Lett.* **106**, 110403 (2011).
- [76] H. Shi, S. Chiesa, and S. Zhang, Ground-state properties of strongly interacting Fermi gases in two dimensions, *Phys. Rev. A* **92**, 033603 (2015).
- [77] L. He, H. Lü, G. Cao, H. Hu, and X.-J. Liu, Quantum fluctuations in the BCS-BEC crossover of two-dimensional Fermi gases, *Phys. Rev. A* **92**, 023620 (2015).
- [78] A. Niroula, G. Rai, S. Haas, and S. Kettemann, Spatial BCS-BEC crossover in superconducting p - n junctions, *Phys. Rev. B* **101**, 094514 (2020).
- [79] S. Suman, R. Sensarma, and M. Randeria (unpublished).